

Bioinspired Navigation in Shape Morphing Micromachines for Autonomous Targeted Drug Delivery

Hen-Wei Huang, Sean Lyttle and Bradley J. Nelson

Abstract—Soft micromachines made out of stimuli-responsive hydrogels have the potential to emulate the navigation strategy of leukocytes to implement autonomous targeted drug delivery. Leukocytes navigate in their natural environment with a variety of strategies in response to chemical gradients. They can detect gradients and redirect their movement towards the gradient source, or adjust their speed while moving up-gradient through cell body morphing known as cell polarization. In this work, we use thermo-responsive hydrogels to engineer self-folding micromachines that can sense near infrared (NIR) light gradients and react in a morphing manner to adjust their speed. We load drug molecules into the unfolded micromachines and encapsulate the drug by folding the micromachines at body temperature. A location of interest is targeted with an NIR light, and a rotating magnetic field is applied to navigate the microrobots to explore the region. Results from *in vitro* experiments demonstrate that the robots speed up while moving up-gradient, automatically stop at the location of interest, and start to release the encapsulated drug molecules by unfolding their shape. The autonomous navigation is achieved without any external imaging feedback by coordinating the sensory input and shape morphing output of the microrobots through the single degree of freedom (DOF) shape control.

I. INTRODUCTION

Targeted drug delivery enables a clinician to control the concentration of medicine in a target region directly. This means of delivery is largely founded on nanomedicine, which employs nanoparticles as vehicles to carry therapeutic agents directly to diseased tissue, thereby avoiding negative effects on healthy tissue [1], [2]. However, these nanoparticles usually lack active mobility, which means they must rely on blood circulation to approach target areas. This is a problem because a drug's success is directly associated with limited circulation time in the human body [3].

A variety of micromachines with diverse actuation strategies, for instance magnetic fields [4], structured light [5], acoustics [6], [7], and bacteria [8], have been developed to enable active mobility at low Reynolds number. Many targeted interventions, such as delivering therapeutic agents to a single cell for gene therapy [9], *in vivo* biopsy by microgripper [10], and targeted cell delivery [11] employ magnetic actuation in virtue of its versatile modes and precise, high DOF control, as well as the fact that the human body does not interact with magnetic fields. To implement these applications *in vivo*, the navigation of microrobots towards target sites must rely on reliable imaging feedback for localization, such as computerized tomography (CT) scan or

The authors are with the Institute of Robotics and Intelligent Systems, ETH Zurich, 8092, Zurich, Switzerland. Email: hhuang@ethz.ch, bnelson@ethz.ch

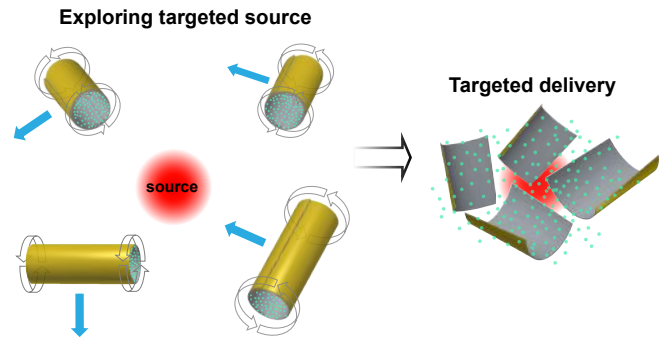


Fig. 1. Schematics of multiple shape morphing microrobots exploring the environment and eventually accumulating at the targeted source to release drugs.

magnetic resonance imaging (MRI). However, accurate, real-time localization of microrobots and targets in the human body remains a major challenge [12]. Moreover, prolonged exposure to X-ray radiation raises the risk of cancer, cardiovascular disease and other non-cancerous diseases [13].

Robots at macro scales capable of integrating sensors, actuators and central controllers can directly form a closed-loop system to realize autonomous navigation without external imaging for localization. At small scales, the conventional sensing, actuating, and computing elements can not be integrated into one single machine. The emerging field of soft robotics provides an alternative that uses morphological computation to facilitate control and perception [14], [15]. Offloading computation from the central controller to the body is achieved by interpreting or transforming the sensory input into shape morphing output. This allows us to encode automation directly into stimuli-responsive materials and structures [16], [17].

This work describes self-folding micromachines based on thermo-responsive hydrogels to implement autonomous targeted drug delivery by emulating the navigation strategy of leukocytes [18]. Drug molecules are loaded in the hydrogel of the initially folded micromachines at room temperature and encapsulated by refolding the microrobots at body temperature to shield the drug from the environment. The microrobots are embedded with magnetic nanoparticles (MNPs), which enables magnetic navigation and NIR triggering shape changes. A location of interest inside human body can be localized first by conventional medical imaging approaches. We then use an NIR light to target the location. Several micromachines can be approximately delivered at the targeted location through needle injection. A rotating magnetic field

is subsequently applied to navigate multiple micromachines to explore the area with the location of interest. These micromachines increase their velocity as approaching the NIR targeted location, autonomously stop moving at the targeted location by unfolding their shape, and begin to release the encapsulated drugs.(Fig. 1).

II. MATERIALS AND METHODS

High water content hydrogels are inherently biocompatible; thus they are widely investigated in a variety of biomedical applications and particularly well-suited to drug delivery applications [19]. However, the high swelling property of hydrogels usually results in a severe leakage of medicine during transport to target sites. In our previous work [20], we developed a novel method using hydrogel bilayer structures capable of drug loading at room temperature and encapsulation at body temperature to prevent the leakage of medicine from a highly swollen hydrogel during transport. In this work, a similar hydrogel-based structure was employed to achieve autonomous targeted drug delivery. The bilayer structure comprises a supporting layer and a drug-loaded layer. Both layers are thermo-responsive but have different thermal swelling characteristics. The supporting layer is embedded with MNPs, enabling magnetic and NIR actuation. The drug-loaded layer stores and releases the drug molecules.

A. Fabrication of hydrogel bilayers

The drug-loaded layer was designed to swell considerably at room temperature (25°C) and less at body temperature (37°C). N-Isopropylacrylamide (NIPAAm) was used as the thermally responsive monomer, whereas polyethylene glycol diacrylate (PEGDA) was used as a cross-linker. A hydrophilic copolymer (Acrylamide, AAm) was used to modify the lower critical solution temperature (LCST) of the NIPAAm. Above LCST, hydrogels no longer swell. The molar ratio between NIPAAm, AAm, and PEGDA was 90:10:0.5, which results in an LCST of 37°C. The photo-initiator 2, 2 dimethoxy 2 phenyl acetophenone (99%, EMPA), and the solvent ethyl lactate was added at a quantity of 3 wt% and 70 wt% the weight of NIPAAm-PEGDA with the aid of an ultrasonic bath over a period of 20 min. The supporting layer had the same material composition as the drug-loaded layer, but different molar ratio between NIPAAm: AAm: PEGDA of 85:15:2, whereas the LCST was 45°C. The photo-initiator and solvent were added in the same proportions as in the drug-loaded layer. MNPS of amorphous Fe₃O₄ with a diameter of 30 nm were dispersed in the supporting layer pre-gel solution at 0.5 vol%. Bilayer structures were obtained by a two-step backside exposure photolithography process [21]. When the bilayer structures were immersed in water at room temperature, they self-folded into a tubular configuration, with the greater part of the drug-loaded layer exposed to the environment.

B. Single DOF shape control of the hydrogel bilayer

Self-folding hydrogel bilayer structures can unfold and refold by increasing the temperature. A modified mathematic

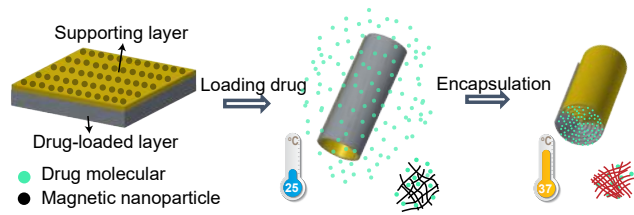


Fig. 2. Schematics of the bilayer structure for drug loading and encapsulation.

model based on Timoshenko bimorph beam theory can be used to estimate the folding curvature of the bilayer structure at various temperatures.

$$\kappa(T) = \frac{6\varepsilon(1+m)^2}{(h_1+h_2)(8(1+m)^2) + (1+m\eta)(m^2 + \frac{1}{m\eta})} \quad (1)$$

where ε is the difference in expansion coefficient between the supporting layer and drug-loaded layer, h_1 is the thickness of the supporting layer, h_2 is the thickness of the drug-loaded layer, η and m are the ratios between the two layers of the elastic modulus and thickness, respectively.

C. Drug loading and release

The self-folded bilayers were immersed and incubated in a thermostatic water bath at body temperature for five minutes to dehydrate the drug-loaded layer. Subsequently, they were immersed in a 1 mM brilliant green (BG) solution at room temperature and were allowed to absorb the model drug for one hour. The BG solution was heated to 37°C to encapsulate the BG in the drug-loaded layer (Fig. 2). Prior to measuring the release of the bilayers at body temperature, they were taken out from the BG solution and immersed in DI water for 1 minute to rinse off any residual BG on the surface. Then, the bilayers were immersed in 300 μ L PBS solution within an Eppendorf, and the release of the embedded BG was monitored at body temperature for one hour. The PBS solution and any released BG was collected, measured, and replaced with fresh PBS solution every five minutes.

Simulations conducted by COMSOL Multiphysics® 5.2 with the model of transport and adsorption were used to elucidate the influence of geometry on molecule diffusion. The physics of transport of diluted species was studied in a time dependent case. Geometries such as a square plate, a hollow tube with the drug-loaded layer on the outer side, and a hollow tube with the drug-loaded layer on the inner side, were employed in the solid models.

D. Bioinspired navigation strategies

A variety of environmental cues can attractively or repulsively guide many types of cells. For instance, unicellular organisms can find resources or avoid predators through migration in response to chemical gradients, such as pH or oxygen. In multi-cellular organisms, directed cell migration underlies development, regeneration, and immune control. Various responses of cells observed in gradients can be viewed as navigational solutions with a trade-off between

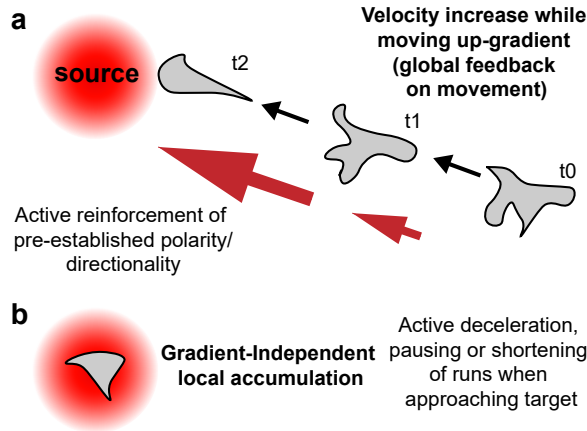


Fig. 3. Bioinspired navigation strategy. (a) Adjustment of directional speed along gradient. (b) Slowing down at the source. Black arrows represent transitions in time and red arrows represent cell movement.

gradient reading accuracy and exploratory potential. Cells capable of adjusting their directional speed while moving along a gradient exhibit high exploratory potential but low gradient reading accuracy, but these cells can explore more space through random advancement (Fig. 3a). Another strategy to enhance the exploratory potential is local deceleration at the gradient source; cells can randomly arrive at the target and locally accumulate (Fig. 3b). This is the least demanding strategy for the cells as it makes full use of random exploration of the environment and has no special requirements regarding tissue geometry or gradient shape. In this work, we encode the navigation strategies of enhancing exploratory potential in the shape morphing micromachines.

E. Experimental Setup

Five DOF locomotion of the self-folding micromachines can be achieved by using an eight-coil electromagnetic manipulation system (Octomag). An NIR laser source (wavelength 808 nm, 1.5 W, SLOC lasers, China) is used to define the target site, and also to heat up the micromachines and modulate their shape. The system is capable of generating uniform magnetic fields up to 40 mT and magnetic field gradients up to 1 T/m. All the experiments are performed in a glass Petri dish placed in the middle of the workspace, filled with deionized water at 37°C.

F. Manipulation of micromachines in low Reynolds number flow

Tubular micromachines are subjected to an externally applied magnetic field H with a flux density $B = \mu_0 H$, where μ_0 is the permeability of vacuum. The torque that acts on the micromachines can be described as

$$\tau_T = VM \times B \quad (2)$$

where M is the volume magnetization in [A/m] of the object of volume V . When the micromachine translates and rotates near a surface, it experiences a drag force, which is approximated by assuming that the micromachine is a solid circular cylinder in a low Reynolds number flow perpendicular to its

long axis. Analytical models for the drag force and torque acting on a cylinder in open flow can be found in [22]. If the locomotion occurs in a confined space close to a wall, the drag force is then estimated by

$$F_d/L = \frac{-4\pi\mu_d U}{\log 2k + (\frac{k}{2})^2} \quad (3)$$

where $k = r_c/d_c$ is the fluid's dynamic viscosity and U is the relative velocity between the fluid and the micromachine. The parameters corresponding to the wall interaction are the radius of the cylinder (r_c) and the distance between the center of the micromachine and the wall (d_c). The drag torque on a cylinder rotating close to a wall is given by [23]

$$\tau_d/L = \frac{-4\pi\mu_d \omega r_c^2}{\sqrt{1-k^2}} \quad (4)$$

The translational velocity of the tubular micromachine rolling near a substrate can be described as

$$U = \mu_s r_c \omega \quad (5)$$

where $0 < \mu_s < 1$ is the slip coefficient, which depends on the viscosity of the liquid as well as the characteristics of the surfaces of the micromachine and the substrate.

G. Navigation strategy for autonomous targeted delivery

In this work, we applied a rotating magnetic field to make the microrobots roll on a substrate to move forward. The plane of the rotating magnetic field automatically changed its orientation in 45° increments every 5 s to ensure that the micromachines could explore the whole area. Therefore, the micromachines could only stay in one direction for 5 s. The duration of 5 s is chosen because the micromachines require nearly 5 s to completely unfold. We used an NIR light to target a location of interest. The gradient of the NIR light triggered the unfolding of the micromachines. When the micromachines are on their way towards the targeted location and sensed the NIR gradient, they are encoded to speed up to enhance the chance to reach the targeted area before the orientation of the magnetic field changes. Once the micromachines reach the source of the gradient, their mobility will be disabled, and they will start to release the encapsulated drug by unfolding. If the micromachines cannot reach the source in the direction within 5 s, their moving direction will be reoriented and they will start to explore the area again (Fig. 4).

III. RESULTS AND DISCUSSIONS

Self-folding bilayer structures based on thermo-responsive hydrogels are employed to load, encapsulate, and deliver drugs through a single DOF shape control. Drugs are loaded in the unfolded micromachines at room temperature, encapsulated by folding the micromachines at body temperature and released by unfolding the micromachines at the target site. The MNPs embedded in the supporting layer of the micromachines enable not only the magnetic navigation but also the NIR-triggered shape changes. In the following sections, we will study the shape change, translational speed,

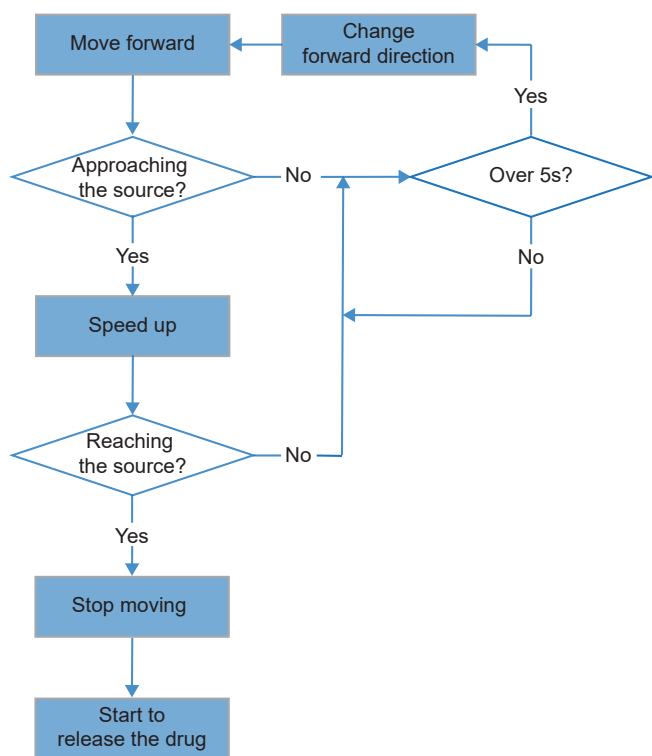


Fig. 4. The flow chart of the navigation strategy for autonomous targeted drug delivery

and sustained drug release of our soft micromachines controlled by temperature variations that can be regulated by an externally applied NIR light.

A. Single DOF shape control

Shape morphing micromachines are achieved by coupling two hydrogels with different thermal swelling characteristics. The inset of Fig. 5 shows the thermal response of the individual supporting layer and drug-loaded layer. The drug-loaded layer has a considerably higher weight swelling ratio (WSR) than the supporting layer at room temperature to ensure the drug-loading capacity. This difference of WSR between the two layers determines the morphology of the bilayer structure that can be controlled by varying temperature. At room temperature, the bilayer forms a tubular configuration with the drug-loaded layer on the outer side, which allows the drug-loaded layer to absorb drug solutions. When increasing the temperature from room temperature to body temperature, the WSR of the drug-loaded layer rapidly decreases, and the gel matrix of the drug-loaded layer entirely collapses, which induces a refolding procedure that switches the drug-loaded layer from the outer side to the inner side. The drug-loaded layer is thereby shielded from the environment by the supporting layer, and the drug molecules are encapsulated in the refolded bilayer. In the meantime, the WSR of the supporting layer decreases only slightly. As the temperature continues to increase from 37°C, the supporting layer gradually dehydrates, triggering the unfolding of the refolded bilayer. At 45°C, the supporting

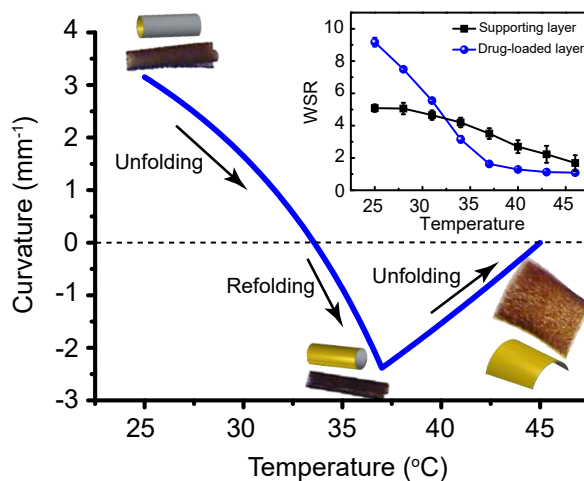


Fig. 5. The temperature response of the curvature of the bilayer structure and the weight swelling ratio (WSR) of the individual layers.

layer entirely dehydrates, and the bilayer fully unfolds. The corresponding folding curvature of the bilayer is obtained by (1) and shown in Fig.5. The curvature of the bilayer structure can be directly controlled by varying the temperature.

B. Shape influence on drug release

Naturally, the shape of self-folded micro-structures influences their drug release characteristics. [24], [25]. We employ the difference in the diffusion of molecules for different shape configurations to implement drug loading, encapsulation, and delivery through temperature-controlled shape-morphing micromachines. Fig. 6 shows the simulation results of the molecule diffusion from the drug-loaded layer of bilayer structures with various configurations to the environment for different configurations. Three different configurations of the micro-structures, which are folded tube, refolded tube and unfolded plate, are analyzed. The folded tube with the drug-loaded layer on the outer side, designed to absorb the drug solution, allows the molecules to leak into the environment (Fig. 6a). The refolded tube with the drug-loaded layer on the inner side, designed to encapsulate the drug, prevents leakage of the drug (Fig. 6b). The unfolded plate, designed to release the encapsulated drug molecules at target sites, exhibits unidirectional drug release (Fig. 6c).

C. Velocity of shape morphing micromachines

The tubular micromachines are driven by external rotating magnetic fields to navigate in low Reynolds number conditions. They roll near the substrate by rotating along their long axis to move forward. The forward velocity is proportional to the rotating radius and frequency, according to (5). Therefore, the speed can be modulated by the single DOF shape control of the micromachines without interfering with the external magnetic field control. The self-folded micromachines are devised to have the smallest possible folding radius at body temperature to minimize drug leakage. Increasing the temperature from 37°C results in increasing the forward velocity of the self-folded micromachines (Fig. 7a). While increasing

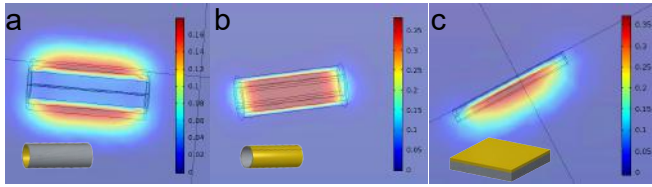


Fig. 6. Simulation results of the drug release at different geometry.

the temperature to increase the speed of the micromachine by enlarging the folding radius, fluid drag forces (3) and torques (4) on the micromachines are also increased, which might decrease the velocity. At low Reynolds number, the applied magnetic torque must be balanced by the induced fluid drag torque. By solving (2) and (4), the maximum rotational speed of the rolling micromachines can be described as

$$\omega_M = \frac{\tau_T \sqrt{1 - k^2}}{L 4\pi\mu_d r_c^2} \quad (6)$$

Under a constant magnetic torque, increasing the radius results in decreasing the rotational speed, until the rotational motion of the micromachines no longer synchronizes with the external magnetic field. As the amplitude of the magnetic field is set at 5 mT, the maximum rotational frequency of the micromachines is 3 Hz at body temperature. At 45°C, the micromachines are completely unfolded, and therefore the forward velocity dramatically drops (Fig. 7a). The mobility of the micromachines is disabled when the rotating frequency of the micromachines is reduced to 0 Hz. We exploit this to enhance the locomotion control of the micromachines. If there is a gradient of temperature, the micromachines can gradually speed up by enlarging the radius while moving up-gradient. Once the micromachines reach the source of the gradient, the temperature at the source can completely unfold the micromachines and disable their mobility.

D. Addressable shape control by NIR targeting

The embedded MNPs in the supporting layer are capable of absorbing and converting NIR light to heat to regulate the temperature of the hydrogel bilayer structure, which in turn controls the shape of the self-folding micromachines. Fig. 7b shows the temperature elevation of the hydrogel bilayers subjected to the NIR light for 15 secs. The temperature on the surface is measured and shows the heating rate is up to 1.7 °C/s. By interpolating, increasing the temperature from 37 °C to 45 °C requires 4 secs, which is then also the time required to disable the mobility of the micromachines. In this manner, the micromachines can sense the NIR light and react by unfolding their tubular shape. By measuring the curvature of the bilayer structure subjected to NIR light, the absorbed energy can be estimated. Therefore, the morphological sensing capability can also facilitate the perception of a gradient of an NIR source. Then, we use the NIR light as an environmental cue to target regions of interest. The micromachines can sense and react to this environmental cue and automatically adjust their shapes to perform specific tasks at the target site.

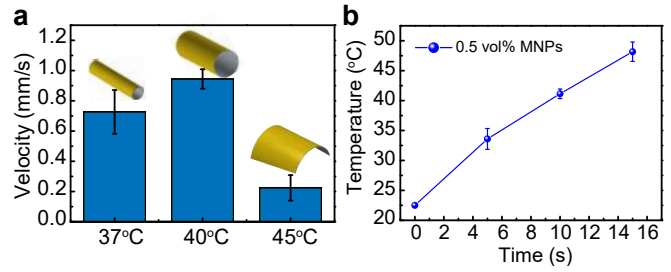


Fig. 7. (a) Velocity of the micromachines versus temperature. The rotating frequency and amplitude of the applied magnetic field is 3 Hz and 5mT. (b) Time response of the temperature elevation of the shape morphing micromachines by applying NIR light.

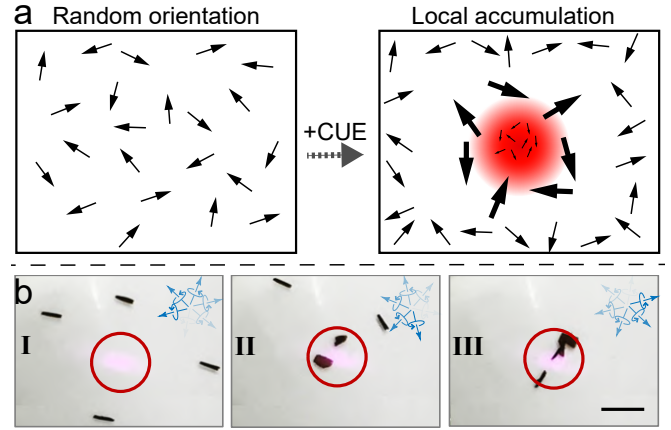


Fig. 8. Collection of micromachines at the NIR targeted region. Black arrows represent the orientation of the microrobots. Blue arrows represent orientation of the rotating magnetic fields. The scale bar is 2mm.

E. Autonomous targeted drug delivery

Soft micromachines made out of programmable materials allow us to program automation directly into their soft body. The proposed shape morphing micromachines can autonomously change their shape to accelerate or decelerate their speed in response to an environmental cue and stop moving to perform targeted intervention without feedback from the external system. Fig. 8a shows four self-folded micromachines navigated by a global rotating magnetic field in random orientations. Without an environmental cue, these micromachines just randomly wander around the area. Once an NIR light is introduced and targets the central region of the environment, the micromachines encoded with the bio-inspired navigation strategy are attracted by the NIR light. As the micromachines approach the NIR source, they speed up, increasing their chance to reach the targeted area. If they arrive in the NIR target area before the orientation of the magnetic field changes, these micromachines will remain at the targeted region to perform the given task. Fig. 8b shows that the four micromachines eventually all reach the NIR target site due to the completely unfolded shape. The unfolded configuration also triggers drug release. Fig.9 shows the difference in the accumulated release between the refolded and unfolded configuration of the micromachines. The drug encapsulated in the refolded configuration has less

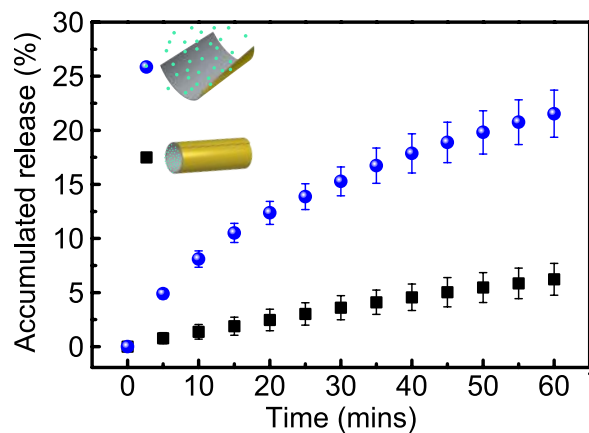


Fig. 9. Drug releases in bilayered tubes at different temperatures.

than 5% leakage within one hour during the transport to the targeted area. When arriving at the targeted area, the micromachines unfold to release the encapsulated drug. The accumulated drug release reaches 20% in one hour.

IV. CONCLUSIONS

Self-folding micromachines made of thermo-responsive hydrogels are able to sense NIR light gradients and react to them by morphing their shape. We encode a navigation strategy inspired by leukocytes in the shape morphing micromachines to implement autonomous targeted drug delivery. Our results suggest that the sophisticated locomotion control, the perception of environmental gradients, and the control of sustained drug release can be facilitated through the single DOF shape control of the self-folding micromachines. We demonstrate that the micromachines can increase their speed while moving up-gradient, automatically stop at the location of interest, and start to release the encapsulated drugs by unfolding their shape without relying on any external imaging feedback.

ACKNOWLEDGMENT

The authors would like to thank Ms. Soomin Lee and Mr. Jonathan Perraudin for their efforts in experiments of drug release. Financial support by the European Research Council Advanced Grant Soft Microrobotics, by the ERC grant agreement n. 743217, and by the Swiss National Science Foundation is gratefully acknowledged.

REFERENCES

- [1] R. Singh and J. W. Lillard, "Nanoparticle-based targeted drug delivery."
- [2] B. J. Nelson, I. K. Kaliakatsos, and J. J. Abbott, "Microrobots for Minimally Invasive Medicine," *Annual Review of Biomedical Engineering*, vol. 12, no. 1, pp. 55–85, 7 2010.
- [3] K. Ulbrich, K. Hola, V. ˇSubr, A. Bakandritsos, J. Tuˇcek, and R. Zbořil, "Targeted Drug Delivery with Polymers and Magnetic Nanoparticles: Covalent and Noncovalent Approaches, Release Control, and Clinical Studies," *Chemical Reviews*, vol. 116, no. 9, pp. 5338–5431, 5 2016.
- [4] Qianwen Chao, Jiangfan Yu, Chengkai Dai, Tiantian Xu, L. Zhang, C. C. Wang, and Xiaogang Jin, "Steering micro-robotic swarm by dynamic actuating fields," in *2016 IEEE International Conference on Robotics and Automation (ICRA)*. IEEE, 5 2016, pp. 5230–5235.

- [5] S. Palagi, A. G. Mark, S. Y. Reigh, K. Melde, T. Qiu, H. Zeng, C. Parmeggiani, D. Martella, A. Sanchez-Castillo, N. Kapernaum, F. Giesselmann, D. S. Wiersma, E. Lauga, and P. Fischer, "Structured light enables biomimetic swimming and versatile locomotion of photoresponsive soft microrobots," *Nature Materials*, vol. 15, no. 6, pp. 647–653, 2 2016.
- [6] D. Ahmed, T. Baasch, B. Jang, S. Pane, J. Dual, and B. J. Nelson, "Artificial Swimmers Propelled by Acoustically Activated Flagella," *Nano Letters*, vol. 16, no. 8, pp. 4968–4974, 8 2016.
- [7] J. Li, T. Li, T. Xu, M. Kiristi, W. Liu, Z. Wu, and J. Wang, "MagnetoAcoustic Hybrid Nanomotor," *Nano Letters*, vol. 15, no. 7, pp. 4814–4821, 7 2015.
- [8] B.-W. Park, J. Zhuang, O. Yasa, and M. Sitti, "Multifunctional Bacteria-Driven Microswimmers for Targeted Active Drug Delivery," *ACS Nano*, p. acsnano.7b03207, 9 2017.
- [9] F. Qiu, S. Fujita, R. Mhanna, L. Zhang, B. R. Simona, and B. J. Nelson, "Magnetic Helical Microswimmers Functionalized with Lipoplexes for Targeted Gene Delivery," *Advanced Functional Materials*, vol. 25, no. 11, pp. 1666–1671, 3 2015.
- [10] E. Gultepe, J. S. Randhawa, S. Kadam, S. Yamanaka, F. M. Selaru, E. J. Shin, A. N. Kalloo, and D. H. Gracias, "Biopsy with Thermally-Responsive Untethered Microtools," *Advanced Materials*, vol. 25, no. 4, pp. 514–519, 2013.
- [11] S. Fusco, M. S. Sakar, S. Kennedy, C. Peters, R. Bottani, F. Starsich, A. Mao, G. A. Sotiropoulos, S. Pane, S. E. Pratsinis, D. Mooney, and B. J. Nelson, "An integrated microrobotic platform for on-demand, targeted therapeutic interventions," *Advanced Materials*, vol. 26, no. 6, pp. 952–957, 2014.
- [12] A. Servant, F. Qiu, M. Mazza, K. Kostarelos, and B. J. Nelson, "Controlled In Vivo Swimming of a Swarm of Bacteria-Like Microrobotic Flagella," *Advanced Materials*, vol. 27, no. 19, pp. 2981–2988, 5 2015.
- [13] K. Kamiya, "Long-term effects of radiation exposure on health," *The Lancet*, vol. 386, no. 9992, pp. 469–478, 2015.
- [14] V. C. Muller and M. Hoffmann, "What Is Morphological Computation? On How the Body Contributes to Cognition and Control."
- [15] D. Rus and M. T. Tolley, "Design, fabrication and control of soft robots," *Nature*, vol. 521, no. 7553, pp. 467–475, 2015.
- [16] O. M. Wani, H. Zeng, A. Priimagi, V. P. Tondiglia, and T. J. White, "A light-driven artificial flytrap," *Nature Communications*, vol. 8, no. May, p. 15546, 2017.
- [17] M. A. McEvoy and N. Correll, "Materials that couple sensing, actuation, computation, and communication," *Science*, vol. 347, no. 6228, pp. 1 261 689–1 261 689, 2015.
- [18] M. Sarris and M. Sixt, "Navigating in tissue mazes: chemoattractant interpretation in complex environments," *Curr. Opin. Cell Biol.*, vol. 36, pp. 93–102, 2015.
- [19] T. R. Hoare and D. S. Kohane, "Hydrogels in drug delivery: Progress and challenges," *Polymer*, vol. 49, no. 8, pp. 1993–2007, 2008.
- [20] H.-W. Huang, A. J. Petruska, M. S. Sakar, M. Skoura, F. Ullrich, Q. Zhang, S. Pane, and B. J. Nelson, "Self-folding hydrogel bilayer for enhanced drug loading, encapsulation, and transport," in *2016 38th Annual International Conference of the IEEE Engineering in Medicine and Biology Society (EMBC)*. IEEE, 8 2016, pp. 2103–2106.
- [21] H.-W. Huang, M. S. Sakar, K. Riederer, N. Shamsudhin, A. Petruska, S. Pane, and B. J. Nelson, "Magnetic microrobots with addressable shape control," in *(ICRA), 2016 IEEE International Conference on Robotics and Automation*, Stockholm, Sweden, 2016.
- [22] Y. Takaisi, "Note on the Drag on a Circular Cylinder moving with Low Speeds in a Semi-infinite Viscous Liquid bounded by a Plane Wall," *Journal of the Physical Society of Japan*, vol. 11, no. 9, pp. 1004–1008, 9 1956.
- [23] S. Champmartin, A. Ambari, and N. Rousset, "Flow around a confined rotating cylinder at small Reynolds number," *Physics of Fluids*, vol. 19, no. 10, p. 103101, 10 2007.
- [24] S. Fusco, H.-W. Huang, K. E. Peyer, C. Peters, M. Haberli, A. Ulbers, A. Spyrogiani, E. Pellicer, J. Sort, S. E. Pratsinis, B. J. Nelson, M. S. Sakar, and S. Pane, "Shape-switching microrobots for medical applications: The influence of shape in drug delivery and locomotion," *ACS Applied Materials & Interfaces*, vol. 7, pp. 6803–6811, 2015.
- [25] K. Malachowski, J. Breger, H. R. Kwag, M. O. Wang, J. P. Fisher, F. M. Selaru, and D. H. Gracias, "Stimuli-responsive theragrippers for chemomechanical controlled release," *Angewandte Chemie - International Edition*, vol. 53, no. 31, pp. 8045–8049, 2014.